

# Crystallographic and magnetostriction properties of Fe and FeB-alloy thin films formed on MgO(100) single-crystal substrates

Y. Asai, T. Kawai, M. Ohtake, and M. Futamoto

Faculty of Science and Engineering, Chuo University, 1-13-27 Kasuga, Bunkyo-ku, Tokyo, 112-8551, Japan

**Abstract.** Fe(100)<sub>bcc</sub> single-crystal film, Fe-B amorphous film, and Fe-B film consisting of a mixture of epitaxial bcc(100) crystal and amorphous are prepared on MgO(100) single-crystal substrates. The influence of crystallographic property on the magnetostriction behavior under rotating magnetic fields is investigated. The output waveform of magnetostriction is sinusoidal for the amorphous film, whereas that of single-crystal film shows a triangle shape. 90° magnetic domain walls are observed for the single-crystal Fe film and the film shows a four-fold symmetry in in-plane magnetic anisotropy. The observation of triangle waveforms is related to the domain wall motion in magnetically unsaturated Fe(100)<sub>bcc</sub> film under rotating magnetic fields. A distortion from triangle wave is observed for the Fe-B film consisting of a mixture of bcc-crystal and amorphous. The magnetostriction behavior is influenced by the magnetization structure.

## 1 Introduction

Soft magnetic materials have been widely used in applications like transformers, motors, and magnetic devices, where the materials are often exposed to alternating magnetic fields. In order to apply soft magnetic materials for such practical applications, it is important to understand the magnetostriction behavior under rotating magnetic fields. However, there are few reports on the magnetostriction behavior under rotating fields [1–3]. The magnetostriction is considered to be influenced by the magnetic anisotropy and the crystallographic property of the material.

Fe and FeB-alloy are typical soft materials. As the B content increases, the crystallographic structure of FeB-alloy varies from bcc-crystal to amorphous. In order to investigate the magnetostriction of materials with magnetic anisotropies, it is useful to employ an epitaxial single-crystal thin film, because the film uniformity and the magnetic anisotropy are controlled by the orientation of single-crystal substrate. In our previous study [4], the effects of Fe/B composition and formation temperature on the crystallographic properties of FeB-alloy films were investigated. In the present study, Fe(100) single-crystal film, FeB amorphous film, and FeB film consisting of a mixture of bcc(100) crystal and amorphous are prepared on single-crystal substrates by adjusting the Fe/B composition and the substrate temperature. The relationship between crystallographic property and magnetostriction behavior under rotating fields is investigated.

## 2 Experimental procedure

Thin films were prepared on polished MgO(100) substrates by using a radio-frequency (RF) magnetron sputtering system equipped with a reflection high-energy electron diffraction (RHEED) facility. The base pressures were lower than  $4 \times 10^{-7}$  Pa. The thickness of MgO substrate was 500  $\mu\text{m}$ . Before film formation, substrates were heated at 600 °C for 1 h in the ultra-high vacuum chamber to obtain clean surfaces. The surface structure was checked by RHEED. Figure 1(a) shows the RHEED pattern observed for an MgO(100) substrate after heating. The diffraction pattern corresponds to a clean MgO surface, as shown in the spot map of figure 1(e).

Three kinds of films with different crystallographic properties were prepared by adjusting the Fe/B composition and the substrate temperature. An Fe film consisting of epitaxial bcc-crystal, an Fe<sub>87</sub>B<sub>13</sub> (at. %) film consisting of a mixture of epitaxial bcc-crystal and amorphous, and an Fe<sub>75</sub>B<sub>25</sub> film consisting of amorphous were formed on MgO substrates at 300, 400, and 300 °C, respectively. The film thickness was fixed at 500 nm.

The surface structure was studied by RHEED. The structural properties were investigated by X-ray diffraction (XRD) with Cu-K $\alpha$  radiation (wave length: 0.15418 nm). The magnetization curves were measured by using a vibrating sample magnetometer. The magnetostriction was measured by cantilever method using a laser displacement meter under rotating magnetic fields up to 1000 Oe [5]. Saturation magnetostriction,  $\lambda_s$ , is calculated by a formula,

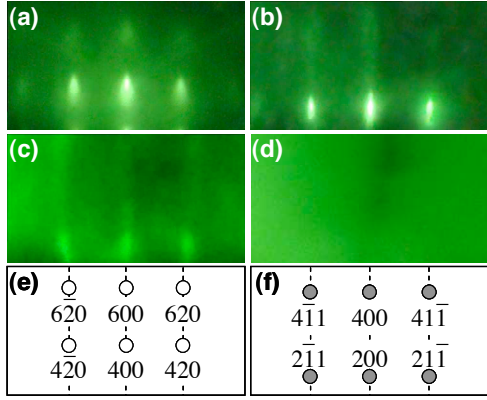


**Fig. 1.** (a)–(d) RHEED patterns observed for (a) an MgO(100) substrate and (b) Fe, (c) Fe<sub>87</sub>B<sub>13</sub>, and (d) Fe<sub>75</sub>B<sub>25</sub> films grown on MgO(100) substrates. The incident electron beam is parallel to MgO[001]. (e, f) RHEED spot maps corresponding to (e) B1(100) and (f) bcc(100) surfaces.

$$\lambda_s = \frac{\Delta S \times t_s^2}{3 \times L^2 \times t_f} \times \frac{E_s \times (1 + \nu_f)}{E_f \times (1 - \nu_s)}, \quad (1)$$

where  $\Delta S$  is the measured bending,  $L$  is the distance between laser beam points,  $t$  is the thickness,  $E$  is Young's modulus,  $\nu$  is Poisson's ratio, and the subscripts of  $f$  and  $s$  respectively refer to film and substrate.

### 3 Results and discussion

Figure 1(b) shows the RHEED pattern observed for an Fe film grown on MgO(100) substrate. A clear diffraction pattern corresponding to bcc(100) single-crystal surface is observed, as shown in the RHEED spot map of figure 1(f). A bcc(100) single-crystal film is obtained. The epitaxial orientation relationship is determined by RHEED as

$$\text{bcc}(100)[011] \parallel \text{MgO}(100)[001].$$

The bcc(100) lattice is rotated around the film normal by 45° with respect to the MgO(100) lattice. In this configuration, the lattice mismatch between Fe film and MgO substrate is -3.7%. Figure 1(c) shows the RHEED pattern observed for an Fe<sub>87</sub>B<sub>13</sub> film. A diffuse RHEED reflection typical for amorphous structure is overlapped with the bcc(100) reflection. The Fe<sub>87</sub>B<sub>13</sub> film involves amorphous in addition to the epitaxial bcc(100) crystal. Figure 1(d) shows the RHEED pattern observed for an Fe<sub>75</sub>B<sub>25</sub> film. No RHEED reflections from bcc-crystals are recognized. An amorphous film is formed. The crystallographic properties are apparently varied by the Fe/B composition and the substrate temperature. Figures 2(a-1)–(c-1) and 3(a-1)–(c-1) show the out-of-plane and the in-plane XRD spectra of Fe, Fe<sub>87</sub>B<sub>13</sub>, and Fe<sub>75</sub>B<sub>25</sub> films, respectively. The in-plane XRDs are measured by making the scattering vector parallel to MgO[011] direction. For the Fe and the Fe<sub>87</sub>B<sub>13</sub> films, bcc(200) reflections are observed in the out-of-plane spectra, whereas bcc(002) reflections are recognized in the in-plane spectra. The XRD result confirms the epitaxial

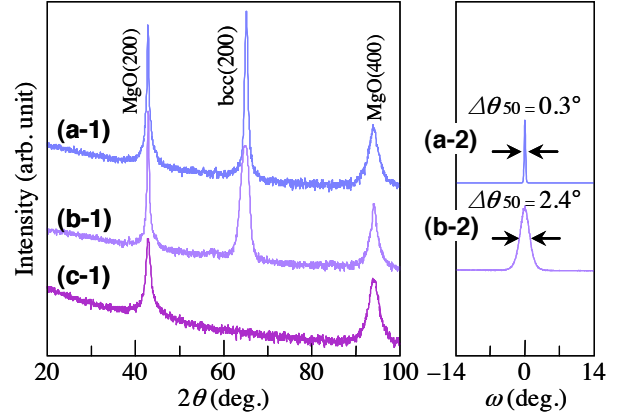


**Fig. 2.** (a-1)–(c-1) Out-of-plane XRD spectra of (a-1) Fe, (b-1) Fe<sub>87</sub>B<sub>13</sub>, and (c-1) Fe<sub>75</sub>B<sub>25</sub> films grown on MgO(100) substrates. (a-2, b-2) Rocking curves measured for bcc(200) reflection peaks in (a-1, b-1), respectively. The intensity is shown in (a-1)–(c-1) a logarithmic or (a-2, b-2) a linear scale.

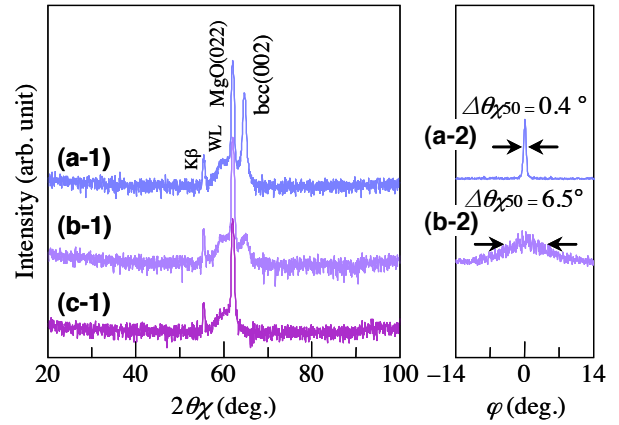


**Fig. 3.** (a-1)–(c-1) In-plane XRD spectra of (a-1) Fe, (b-1) Fe<sub>87</sub>B<sub>13</sub>, and (c-1) Fe<sub>75</sub>B<sub>25</sub> films grown on MgO(100) substrates. The scattering vector of in-plane XRD is parallel to MgO[011]. (a-2, b-2) Rocking curves measured for bcc(002) reflection peaks in (a-1, b-1), respectively. The intensity is shown in (a-1)–(c-1) a logarithmic or (a-2, b-2) a linear scale.

orientation relationship determined by RHEED. The intensities of bcc(200) and bcc(002) reflections from Fe<sub>87</sub>B<sub>13</sub> film are weaker than those from Fe film. This is due to that the Fe<sub>87</sub>B<sub>13</sub> film consists of a mixture of epitaxial bcc-crystal and amorphous. For the Fe<sub>75</sub>B<sub>25</sub> film, reflections from bcc crystals are absent, because the film structure is amorphous.

The in-plane and the out-of-plane lattice constants of  $a$  and  $c$  are respectively calculated by using the relations,  $a = 2d_{\text{bcc}(200)}$  and  $c = 2d_{\text{bcc}(002)}$ . The ( $a$ ,  $c$ ) values of Fe and Fe<sub>87</sub>B<sub>13</sub> films are (0.2864 nm, 0.2884 nm) and (0.2874 nm, 0.2880 nm), respectively. The  $c$  values are 0.7% and 0.2% larger than the  $a$  values for the Fe and the Fe<sub>87</sub>B<sub>13</sub> films, respectively. The reason is possibly due to accommodation of lattice mismatch between film and substrate. Rocking curves ( $\omega$ - and  $\varphi$ -scan spectra) of out-of-plane and in-plane lattices were measured by fixing the diffraction angles ( $2\theta$  and  $2\theta_\chi$ ) at the peak angles of bcc(200) and bcc(002) reflections, respectively. Figures 2(a-2, b-2) and 3(a-2, b-2) show the rocking curves

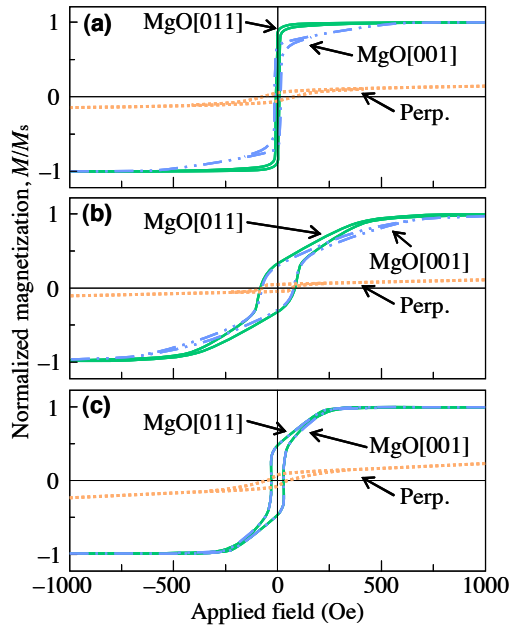
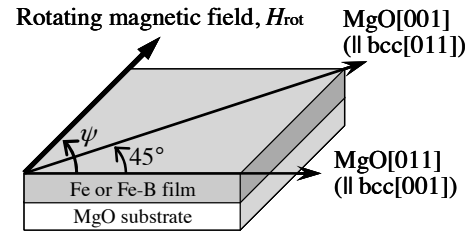


**Fig. 4.** Magnetization curves measured for (a) Fe, (b)  $\text{Fe}_{87}\text{B}_{13}$ , and (c)  $\text{Fe}_{75}\text{B}_{25}$  films grown on MgO(100) substrates.

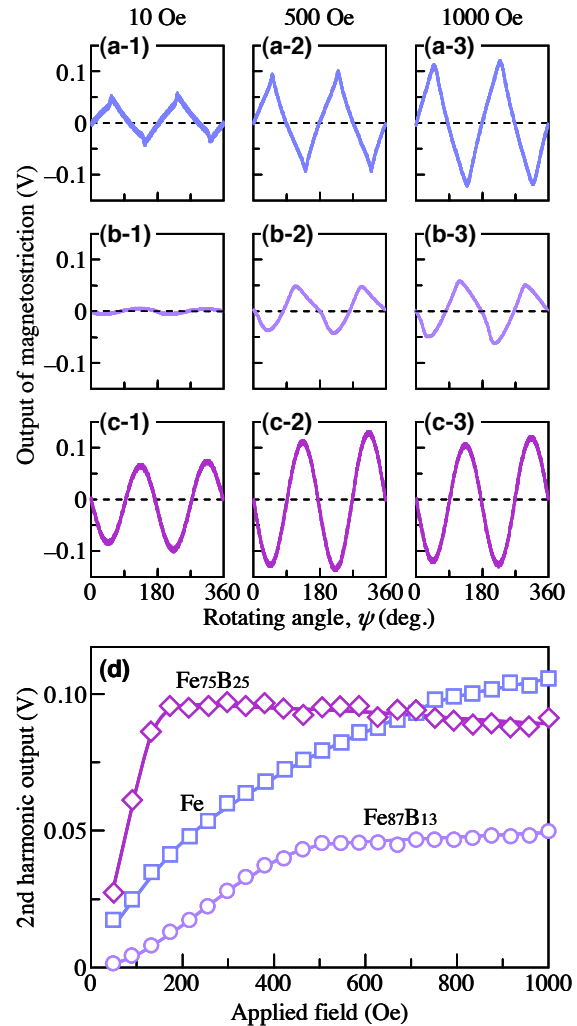
measured for the Fe and the  $\text{Fe}_{87}\text{B}_{13}$  films. The values of full width at half maximum of out-of-plane and in-plane rocking curves,  $\Delta\theta_{50}$  and  $\Delta\theta\chi_{50}$ , of Fe film are  $0.3^\circ$  and  $0.4^\circ$ , while those of  $\text{Fe}_{87}\text{B}_{13}$  film are  $2.4^\circ$  and  $6.5^\circ$ , respectively. The orientation dispersion of  $\text{Fe}_{87}\text{B}_{13}$  film is larger than that of Fe film, possibly due to an influence of interstitial B atom.

Figure 4 shows the magnetization curves. The Fe(100) single-crystal film is easily magnetized when the magnetic field is applied along MgO[011] ( $\parallel$  bcc[001]) direction, while the magnetization curve measured along MgO[001] ( $\parallel$  bcc[011]) direction saturates at a higher applied field. The in-plane magnetization property is considered to be reflecting the magnetocrystalline anisotropy of bulk bcc-Fe crystal with the easy magnetization axes parallel to bcc<100> directions. For the  $\text{Fe}_{87}\text{B}_{13}$  film consisting of epitaxial bcc(100) crystal and amorphous, easy magnetization direction is also observed along MgO[011] ( $\parallel$  bcc[001]) direction. The  $\text{Fe}_{75}\text{B}_{25}$  film shows isotropic in-plane magnetic property due to that the film consists of amorphous structure. The  $\text{Fe}_{87}\text{B}_{13}$  film shows a higher coercivity, when compared with the cases of Fe and  $\text{Fe}_{75}\text{B}_{25}$  films. This is possibly due to suppression of domain wall motion by the presence of boundaries between bcc-crystal and amorphous. The magnetic properties are influenced by the film structure.

Magnetostriction is measured by applying a rotating magnetic field,  $H_{\text{rot}}$ , to a film, as shown in figure 5. Figures 6(a)–(c) show the output waveforms of magnetostriction measured under rotating fields of 10, 500, and 1000 Oe. Triangle waveforms are recognized for the Fe and the  $\text{Fe}_{87}\text{B}_{13}$  films [figures 6(a, b)], whereas usual sinusoidal waveforms are observed for the  $\text{Fe}_{75}\text{B}_{25}$  film [figure 6(c)]. Figure 6(d) shows the dependences of magnetic field on 2nd harmonic outputs measured for the Fe, the  $\text{Fe}_{87}\text{B}_{13}$ , and the  $\text{Fe}_{75}\text{B}_{25}$  films. As the field



**Fig. 5.** Schematic model showing the rotating angle,  $\psi$ , of applied magnetic field with respect to crystallographic orientation of MgO substrate.



**Fig. 6.** (a)–(c) Output waveforms of magnetostriction of (a) Fe, (b)  $\text{Fe}_{87}\text{B}_{13}$ , and (c)  $\text{Fe}_{75}\text{B}_{25}$  films measured under rotating magnetic fields of (a-1)–(c-1) 10, (a-2)–(c-2) 100, and (a-3)–(c-3) 1000 Oe. (d) Dependences of applied magnetic field on 2nd harmonic outputs measured for Fe,  $\text{Fe}_{87}\text{B}_{13}$ , and  $\text{Fe}_{75}\text{B}_{25}$  films.

increases, the output increases for the Fe and the  $\text{Fe}_{87}\text{B}_{13}$  films. This result indicates that the films are not magnetically saturated under a field of 1000 Oe. For the  $\text{Fe}_{75}\text{B}_{25}$  film, the output is kept constant at 0.087 V beyond 200 Oe, where the magnetization is saturated and the  $\lambda_s$  value is calculated by using the equation (1) to be  $5.4 \times 10^{-5}$ .

The triangle magnetostriction behavior will be explained by considering the magnetization structure

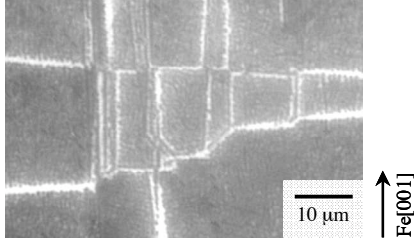


**Fig. 7.** Bitter image observed for an Fe(100) single-crystal film.

variation when the sample is exposed to a rotating field. When the magnetization of a film with a four-fold symmetry in in-plane magnetic anisotropy is not saturated, magnetic domains with  $90^\circ$  walls are generally formed. In the cases of Fe and Fe<sub>87</sub>B<sub>13</sub> films, the magnetization directions in  $90^\circ$  domain structure are considered to be along bcc[010] and bcc[001]. Figure 7 shows the Bitter image observed for the Fe film.  $90^\circ$  magnetic domains are clearly observed. By considering a simplified model of  $90^\circ$  domain structure under a rotating field shown in figure 8, the magnetizations along bcc[010] and bcc[001] ( $M_{[010]}$  and  $M_{[001]}$ ) directions are respectively given by

$$M_{[010]} = M \cos \alpha, \quad (2)$$

$$M_{[001]} = M \sin \alpha, \quad (3)$$

where  $\alpha$  is angle of magnetization direction with respect to bcc[010]. Free energy of the whole system is consisting of an anisotropy energy and the energy supplied from rotating magnetic field. The free energy is given by

$$E = M \cos \alpha (-H_k - H_{\text{rot}} \cos \psi) + M \sin \alpha (-H_k - H_{\text{rot}} \sin \psi), \quad (4)$$

where  $E$  is the free energy,  $M$  is the magnetization, and  $H_k$  is the anisotropy field. In this case, the magnetization orientation is determined so that the free energy becomes minimum. Therefore,

$$\frac{dE}{d\alpha} = 0. \quad (5)$$

By solving the equations (4) and (5) for  $\alpha$ , the  $M_{[010]}$  and  $M_{[001]}$  are given by

$$M_{[010]} = M \cdot \frac{1 + h \cdot \cos \psi}{\sqrt{(1 + h \cdot \sin \psi)^2 + (1 + h \cdot \cos \psi)^2}}, \quad (6)$$

$$M_{[001]} = M \cdot \frac{1 + h \cdot \sin \psi}{\sqrt{(1 + h \cdot \sin \psi)^2 + (1 + h \cdot \cos \psi)^2}}. \quad (7)$$

Here,  $h$  is given by

$$h = \frac{H_{\text{rot}}}{H_k}. \quad (8)$$

The output of magnetostriction is proportional to ( $M_{[010]} - M_{[001]}$ ), and the variations are calculated as a function of rotation angle assuming  $h = 1$ , as shown in figure 9. The magnetostriction output is shown in figure 9(b), which is similar to that of the present experimental result.

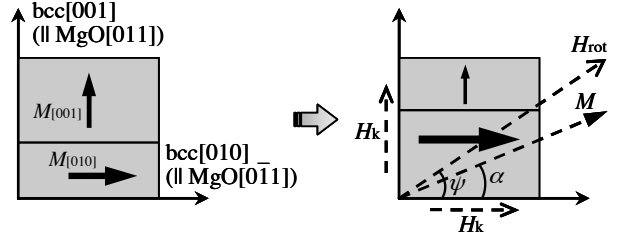


**Fig. 8.** Schematic model showing  $90^\circ$  domain structure under rotating field.

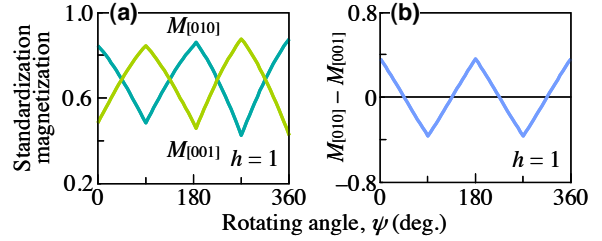


**Fig. 9.** Magnetostriction analysis model of triangle waveform. (a)  $M_{[010]}$  and  $M_{[001]}$ . (b)  $M_{[010]} - M_{[001]}$ .

## 4 Conclusions

Fe single-crystal film, Fe-B amorphous film, and Fe-B film consisting of a mixture of bcc-crystal and amorphous are prepared. The influence of crystallographic property on the magnetostriction behavior under rotating magnetic fields is investigated. The output waveform of magnetostriction under rotating magnetic field measured for the Fe(100) single-crystal film is a triangular shape, while that of amorphous Fe-B film is a sinusoidal shape. The Fe-B film consisting of bcc(100) crystal and amorphous mixture shows a deformed triangular shape. It is shown that the triangular magnetostriction behavior can be explained based on a magnetization structure model considering the  $90^\circ$  magnetic domain wall motion under a rotating magnetic field.

## Acknowledgments

A part of this work was supported by MEXT-Japan and Hattori-Hokokai.

## References

1. M. Enokizono, T. Suzuki, J. D. Sievert, IEEE Trans. Magn. **26**, 2067 (1990)
2. M. Enokizono, S. Kanao, G. Shirakawa, IEEE Trans. Magn. **31**, 3409 (1995)
3. L. Varga, H. Jiang, T. J. Klemmer, W. D. Doyle, IEEE Trans. Magn. **34**, 1441 (1998)
4. Y. Asai, T. Kawai, M. Ohtake, M. Futamoto, Cur. Adv. Mater. Proc. **25**, 463 (2012)
5. T. Kawai, M. Ohtake, M. Futamoto, Thin Solid Films **519**, 8429 (2011)